Lateral Diffusion Coefficients of Separate Lipid Species in a Ternary Raft-Forming Bilayer: A Pfg-NMR Multinuclear Study

Greger Orädd,* Philip W. Westerman,† and Göran Lindblom*
*Department of Chemistry: Biophysical Chemistry, Umeå University, Umeå, Sweden; and †Department of Biochemistry and Molecular Pathology, Northeastern Ohio Universities College of Medicine, Rootstown, Ohio, USA

ABSTRACT By isotopical labeling lipid lateral diffusion coefficients for each of the membrane constituents, including cholesterol, have been measured by ^{1}H, ^{2}H, and ^{19}F pulsed field gradient NMR spectroscopy in macroscopically oriented lipid bilayers. This provides a means of obtaining detailed dynamic and compositional information in raft-forming lipid bilayers without introducing foreign molecules into the systems. The raft systems studied contained dioleoylphosphatidylcholine/dipalmitoylphosphatidylcholine (DPPC)/cholesterol at the molar ratios of 42.5:42.5:15 and 35:35:30 in excess water. At temperatures below 30°C the raft system forms large ($>1\mu$m) domains of a liquid ordered (l_o) phase, in which the lipid lateral diffusion was ~5 times slower than for the lipids in the surrounding liquid disordered (l_d) phase. Within each domain all lipid species showed the same diffusion coefficient, despite the very different structures of cholesterol and phospholipids. DPPC partitions exclusively into the l_o domains, whereas cholesterol and dioleoylphosphatidylcholine were distributed in both l_o and l_d phases. The cholesterol concentration was found to be 10–20 mol % in the l_d domain and 30–40 mol % in the l_o domain. Comparison of these results with data from sphingomyelin-containing systems suggests that DPPC interacts more weakly with cholesterol than does sphingomyelin.

INTRODUCTION

During the past decade the organization of lateral structures in biological membranes and their importance for biological activity have received increasing attention. We have witnessed an emergence of interest in a specific type of microdomain, known colloquially as a membrane raft (1–8), and since the raft concept was coined in 1997, the number of publications on rafts has steadily increased with ~100 articles annually. The raft hypothesis has been stated as a separation of discrete liquid-ordered (l_o) and liquid-disordered (l_d) phase domains that occurs in membranes containing sufficient amounts of sphingolipid and sterol (3), where the l_o phase (9,10) is believed to be rich in sphingomyelin (SM) and cholesterol (CHOL).

Rafts are proposed to be involved in a large number of different cellular processes, including protein sorting (1), signal transduction (11), calcium homeostasis (12), protocytosis (13), alternative routes of endocytosis (14), insulin receptor signaling in adipocytes (15–17), fatty acid translocase (18), and CHOL transport (19). Recently, it was also discovered that the surfactant monolayer of lung alveoli at physiological temperatures forms two fluid phases (20) and it was seen that the lung surfactant proteins tend to accumulate in one type of lipid domain. It has been surmised that CHOL is an important regulator of this domain structure that may have important consequences for the mechanical function of the lung. The lipid dynamics and the lateral membrane structure in this kind of system are being studied in our laboratory at the time of this study, using methods described in this work (G. Orädd, J. Bernadino de la Serna, J. Perez-Gil, and G. Lindblom, G., unpublished).

So far most physicochemical studies of rafts have been performed on model membranes, where it has been demonstrated that mixtures of lipids mimicking the composition of the outer leaflet of plasma membranes exhibit liquid-liquid immiscibility and segregate into l_o and l_d domains. Cell membranes, on the other hand, have an extremely complex lipid composition that may be constituted from ~8 major classes of lipids, including CHOL (21). Thus, the binary and ternary lipid bilayer systems that are studied here can provide only limited, although important, information from which we attempt to extrapolate toward understanding the complexity of cellular membranes. To obtain a detailed insight into the interactions between cholesterol and lipids on the molecular level, it is necessary to deal with model systems. Such knowledge is useful for a comprehension of the function and formation of the different microdomains in complex cell membranes.

A number of different methods has been utilized for studies of liquid-liquid immiscibility in membranes over the years, such as calorimetry (22,23), Langmuir-Blodgett techniques (8,24), AFM (25–27), pulsed-field gradient (pfg-) NMR (28), and in particular various kinds of fluorescence spectroscopy (29–35). The main objection to the latter methods is the need for specific fluorescent probes not usually found in biological systems. The results are thus obtained indirectly via the interactions of the probe molecule with the surrounding membrane and it is desirable to find methods that do not depend on the introduction of foreign molecules. In this regard, the use of NMR in combination

Submitted February 22, 2005, and accepted for publication on April 25, 2005.

Address reprint requests to Göran Lindblom, Tel.: 46-90-7865228; Fax: 46-90-786- 7779; E-mail: goran.lindblom@chem.umu.se.

0006-3495/05/07/315/06 $2.00 doi: 10.1529/biophysj.105.061762

with isotopically labeled molecules is an ideal choice for two reasons: i), this kind of labeling causes minimal changes in the molecular interactions; and ii), the labeling makes it possible to separately study each lipid species with the NMR technique. The use of pfg-NMR to study lipid lateral diffusion in bilayers has proven to be a powerful method in the characterization of domain formation (28,36–38) and in this work we present results obtained by pfg-NMR multinuclear spectroscopy applied on macroscopically aligned bilayers of 1,2-dipalmitoyl-*sn*-glycero-3-phosphocholine (DPPC)/1,2-dioleoyl-*sn*-glycero-3-phosphocholine (DOPC)/CHOL, where DPPC and Chol were labeled with ^{2}H and ^{19}F, respectively. With this unique method, it is possible to determine the lateral diffusion coefficient of all the individual lipids, both within, and outside of, the rafts.

MATERIALS AND METHODS

Preparation of oriented lipid bilayers

The following substances were used for the preparation of macroscopically aligned lipid bilayers; DOPC and 1,2-dipalmitoyl-d_{62}-*sn*-glycero-3-phosphocholine-1,1,2,2-d_4-*N*,*N*,*N*-trimethyl-d_9 (DPPC-d_{75}) were obtained from Avanti Polar Lipids (Birmingham, AL). DPPC, CHOL, deuterated water (^2H_2O), and deuterium depleted water (H_2O) were purchased from Sigma (St. Louis, MO). The ^{19}F-labeled CHOL (25FCH) was synthesized as described previously (39).

Macroscopically oriented bilayers were prepared with excess water after a procedure reported earlier (28). The molar fractions of DOPC and DPPC were held equal, whereas the CHOL contents were 0, 15, and 30 mol %. A lower estimate of the degree of orientation varied from 65 to 85%, as determined from the ^{31}P NMR line shape. The measured lipid diffusion coefficients did not depend on the degree of orientation.

Pulsed field gradient NMR

The diffusion measurements were performed on a Chemagnetics Infinity NMR spectrometer operating at a frequency of 400 MHz for protons equipped with a specifically designed goniometer probe that enable macroscopically aligned bilayers to be oriented with the bilayer normal at the magic angle (54.7°) with respect to the main magnetic field. The temperature was controlled within ±0.5°C by a heated air stream passing the sample. Details of the pfg-NMR method for measurements of lipid lateral diffusion on macroscopically oriented bilayers can be found elsewhere (28).

For all measurements the stimulated spin-echo (STE) pulse sequence was used (40), in which the gradient amplitude, g, was varied while keeping all other parameters constant. The obtained data were analyzed with the CORE method for global analysis of the entire data set (41,42). The analysis was based on the Stejskal-Tanner equation

$$A = \sum_i A_i \exp\left(-\gamma^2\delta^2 g^2 D_i \left(\Delta - \frac{\delta}{3}\right)\right), \qquad (1)$$

where A_i is the spectral amplitudes without applied gradients, γ is the gyromagnetic ratio, Δ is the time interval between gradient pulses, and δ is the duration of the pulsed field gradients. The initial spectral amplitudes A_i are determined by the longitudinal, T_1, and transverse, T_2, NMR relaxation times according to (40)

$$A_i = \frac{I_i}{2} \times \exp\left(\frac{2\tau}{T_{2,i}}\right) \times \exp\left(-\frac{T}{T_{1,i}}\right), \qquad (2)$$

where I is a factor proportional to the proton content in the system, and τ and T are the time intervals determining transverse and longitudinal relaxation, respectively.

The number of diffusion components, i, were varied from 1 to 3 and the sums of the squares of the residuals and inspection of the fits were used to determine the actual number of components appropriate for each measurement. For the proton measurements the fastest diffusion component could be identified with residual water, both from the lineshape and from the large value of the diffusion coefficient (3.2–10.5 × 10^{-10} m^2/s). The remaining signal originates from the phospholipids and could always be described by either one or two components. No signal is expected to remain for CHOL due to the fast relaxation of this molecule. The deuterium data could always be fitted to one component and the fluorine data was fitted to either one or two components. A detailed discussion of the analysis of the experimental data (e.g., the conditions for a lipid diffusion decay consisting of one or two components) is given in a recent report (37).

Measurements were performed in the temperature range 0–60°C, usually in steps of 3°, and starting from the highest temperature. At each temperature several diffusion experiments were performed, in which the diffusion time, Δ, was typically varied from 15 to 100 ms. Some measurements were also performed for $\Delta = 200$ ms on selected samples/temperatures. The obtained diffusion coefficients were not dependent on Δ. However, the relative amplitudes of the separate diffusion components were dependent on Δ, since the relaxation intervals T and τ are changed, affecting the attenuation parameter in Eq. 2. In general, the standard deviation of the lipid diffusion coefficients measured with proton NMR, for several different Δs, was <5% for a fit with one component as well as for the fast component in two component fits, whereas it was typically 20–30% for the slow component in two component fits. Given the small number of measurements, this translates to an approximate absolute error of 0.3 × 10^{-12} m^2/s for all the measurements. For the NMR measurement utilizing ^{19}F and ^{2}H nuclei, only one diffusion experiment was performed at each temperature, since a rather long acquisition time was needed to obtain an acceptable signal/noise ratio. In these cases, a 90% confidence interval for the diffusion coefficients was estimated using the method described in (43). This resulted in confidence intervals of ±5–30% for both the ^{19}F and ^{2}H NMR measurements with the larger intervals at lower temperatures, since then the signal to noise ratio was lowest because of the faster relaxation rates.

RESULTS

Fig. 1 shows the lipid lateral diffusion coefficients for a lipid bilayer with 30 mol % CHOL. For the DOPC/DPPC/CHOL system (*left panel*) the translational diffusion was obtained from ^{1}H NMR measurements (*circles*). For $T > 33$°C the decay is well described by one component, giving a single diffusion coefficient, but for $T \leq 33$°C the diffusion decay splits up into two separate components. No assignment to the two lipids contributing to the signal can be made, because of severe overlap of the signals from DOPC and DPPC. Note that CHOL is not expected to contribute to the spin-echo signal due to the much faster relaxation of this rather rigid molecule. The two components are presented in the figure so that the size of the symbol is proportional to the relative amount of the signal from the respective components. For comparison the left panel also shows the results obtained for the DOPC/SM/CHOL system with equimolar amounts of DOPC and SM and 30 mol % CHOL (*plus signs*, data taken from (37)), and the one component diffusion data for the DOPC/DPPC system (*solid line*).

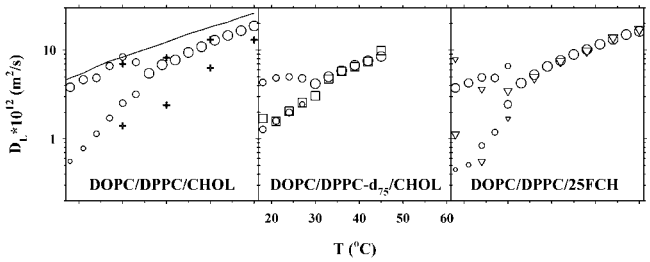

FIGURE 1 Lipid lateral diffusion coefficients obtained for samples with the molar composition 35:35:30 of DOPC/DPPC/CHOL (*left*), DOPC/DPPC-d_{75}/CHOL (*middle*), and DOPC/DPPC/25FCH (*right*). Diffusion data of three nuclei are shown: ^{1}H (*circles*), ^{2}H (*squares*), and ^{19}F (*triangles*). For two-component diffusion, the symbol sizes are proportional to the relative amount of each component. Also shown in the left plot are proton diffusion data for the DOPC/DPPC-d_{75} system (*solid line*) and for the previously published DOPC/SM/30% CHOL system (*plus signs*) (37).

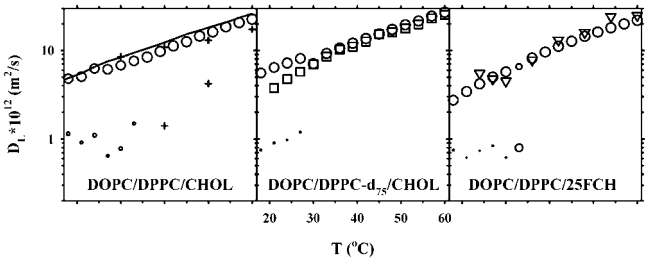

FIGURE 2 Lipid lateral diffusion coefficients obtained for samples with the molar composition 42.5:42.5:15 of DOPC/DPPC/CHOL (*left*), DOPC/DPPC-d_{75}/CHOL (*middle*), and DOPC/DPPC/25FCH (*right*). Diffusion measurements of three nuclei are shown: ^{1}H (*circles*), ^{2}H (*squares*), and ^{19}F (*triangles*). For two-component diffusion, the symbol sizes are proportional to the relative amount of each component. Also shown in the left plot are ^{1}H diffusion data for the DOPC/DPPC-d_{75} system (*solid line*) and for the previously published DOPC/SM/30% CHOL system (*plus signs*) (37).

The middle panel of Fig. 1 shows the diffusion coefficients obtained for the DOPC/DPPC-d_{75}/CHOL system. As can be inferred from this figure for the one-component diffusion region ($T > 27$°C) the diffusion coefficients are equal as measured from either ^{1}H NMR (*circles*) or ^{2}H NMR (*squares*). At the lower temperatures, $T \leq 27$°C, ^{1}H diffusion displays two components, whereas ^{2}H diffusion gives one component, equal in magnitude to the slow component obtained from ^{1}H NMR.

Finally, the right hand panel of Fig. 1 displays the results for the DOPC/DPPC/25FCH system. For $T > 30$°C both ^{1}H NMR (*circles*) and ^{19}F NMR (*triangles*) give one component diffusion, whereas both nuclei display two-component diffusion at temperatures below 30°C. Only three measurements were made with ^{19}F NMR for $T \leq 30$°C, due to the excessive experimental time needed to obtain an acceptable signal for this nucleus. The fast and slow diffusion components are roughly equal for both nuclei, considering the large errors for the fluorine measurements.

In summary, at high temperatures the measured diffusion coefficients are equal in all three samples, and for all three nuclei, but at lower temperatures the proton and fluorine diffusion split into two components, whereas deuterium only shows one component with diffusion equal to the slow component for the other two nuclei.

Fig. 2 displays the corresponding plots for 15 mol % CHOL. For these measurements only very small relative amounts of the slow diffusion component was observed by ^{1}H NMR. Due to the small fraction of this component, the accumulated square sum of the residuals was only marginally improved upon the addition of the second component. However, since the one- to two-component transition occurred at the same temperatures as in Fig. 1, and with diffusion coefficients of comparable magnitude as in this figure, we think it is reasonable to include the second component in this plot. It should be noted that the addition of a second component in the high temperature interval gave unphysical results, such as very small components with diffusion coefficients that were orders of magnitude away from the expected and/or combinations of negative and positive component amplitudes with roughly the same diffusion coefficient. Neither ^{2}H NMR nor ^{19}F NMR revealed more than one component with diffusion, which was equal to the fast component obtained by ^{1}H NMR.

DISCUSSION

High temperature region

In the high temperature region, where only one diffusion coefficient is observed, all lipid molecules diffuse alike, as evidenced by the similar diffusion coefficients obtained by ^{1}H, ^{2}H, and ^{19}F NMR. This indicates that the diffusional motion within the bilayer is governed by some bilayer property rather than by the individual molecular characteristics. According to the free-volume theory the different molecular species will have a similar diffusional motion, if the accessible free volume distribution is the same for all molecules (44). The diffusion coefficients decrease with increasing CHOL content (Figs. 1 and 2). This behavior has been observed in many systems and it is a consequence of the ability of CHOL to reduce the free volume, probably also enhanced by its condensing effect on the hydrocarbon chains of the phospholipids (45).

The immiscibility temperature region

The onset of the region with two-component diffusional motion for protonated lipids is 33°C (Figs. 1 and 2). It seems reasonable to assign the two components to diffusion in the l_o and l_d phases. The immiscibility temperature (T_{mix}) is then in good agreement with investigations by fluorescence microscopy on giant vesicles (29,30). For samples containing DPPC-d_{75}, T_{mix} is reduced by 6°C, also in good agreement with earlier results, in which the reduction in T_{mix} was explained by the lower main transition temperature of

DPPC-d_{75} (29). For samples with 25FCH T_{mix} is the same as for CHOL, indicating that ^{19}F labeling at the 25-position does not appreciably change the physicochemical properties of the CHOL molecule. A CHOL fluorine labeled at the 6-position was also used but, although the qualitative behavior was the same, it was not further used for three reasons: i), the diffusion coefficient was 30–50% higher in the high temperature region; ii), T_{mix} was 9°C lower than for the corresponding CHOL samples; and iii), the signal intensity was much weaker than for 25FCH due to faster spin relaxation. The first two points indicate that the disturbance caused by labeling at the 6-position is larger than for 25FCH, whereas the third point is of mostly practical importance. Furthermore, it has been shown previously that the surface pressure-area isotherm for 25FCH is identical with that of CHOL, whereas that for the 6-labeled CHOL is slightly different from CHOL (39). The finding that a fluorine label in the ring system disturbs the properties of CHOL more than labeling in the hydrocarbon chain is indicative of the importance of the sterol skeleton in raft formation. This has also been suggested in other studies (46) and we are currently performing an investigation involving several biological sterols to gain further insights into the raft-forming mechanism.

Low temperature region, 30 mol % CHOL

First, it should be emphasized that the obtained diffusion coefficients did not depend on the diffusion time when it was varied between 15–200 ms. This implies that the exchange between the two phases is slow on this timescale (37,47). Using the root mean square distance of displacement, $\langle r^2\rangle^{1/2} = (4D\Delta)^{1/2}$, as a measure of the mean distance that the molecules travel during Δ, implies that the size of the aggregates have a lower limit of $\sim$1–2 μm. This is in agreement with fluorescence microscopy results (29,30,48) in which domains >1 μm were observed.

The diffusion coefficient obtained by ^2H NMR closely follows the slow diffusion component measured by ^1H NMR (Fig. 1, *middle panel*). This shows that DPPC is strongly enriched in the l_o phase. It should be noted that generally, the spin relaxation rate in the l_o phase is significantly faster than in the l_d phase, and it can therefore be expected that the NMR signal from the l_d phase is easier to observe than from an l_o phase. Since no evidence of a fast diffusion component could be seen at any temperature in the two-phase region, we conclude that the amount of DPPC residing in the l_d phase must be very small. This result is in slight disagreement with that obtained by Veatch et al. (29), who found small but detectable amounts of DPPC also in the l_d phase.

On the contrary, the diffusion coefficient by ^{19}F NMR splits into a fast and a slow component similarly to the diffusion coefficient obtained by ^1H NMR. This clearly shows that CHOL is distributed into both the l_o and the l_d phases.

The fast proton diffusion coefficient shows a sudden increase as the temperature is dropped below T_{mix} and it is only slightly smaller than that for 0 mol % CHOL (*solid line* in Fig. 1). This indicates that CHOL is more or less depleted from the l_d phase. However, since the data obtained for DPPC-d_{75} indicates that the l_d phase is depleted in DPPC (see below) it is more relevant to compare the lipid diffusion in this phase with that for the DOPC/CHOL system (38) than for the DOPC/DPPC system. A comparison with these data shows that the fast diffusion component is comparable with the diffusion for DOPC bilayers containing 15 mol % CHOL. Using this concentration as one constraint and depletion of DPPC from the l_d phase as a second constraint it is possible to calculate the range of compositions and the relative amounts of the two phases that can form. It turns out that the amount of l_d phase can vary between 0–40% and that the CHOL concentration in the l_o phase is 30–40 mol % within this possible range of two-phase coexistence. It is notable that the amount of CHOL in the l_o phase is close to the upper limit of the l_d/l_o two-phase regions found in binary systems (38,44,49). The choice of 15 mol % CHOL in the l_d phase is not critical for this analysis, similar numbers are obtained also for a choice of 10 or 20 mol %.

The slow diffusion coefficients are 3–7 times smaller than the fast ones and the slow diffusion in this system is slightly higher than in the DOPC/SM/CHOL system reported earlier (37) (Fig. 1, *left panel*, *plus signs*). On the other hand, the general behavior of the diffusion coefficients correlates well between the systems. The onset temperature of the two-component diffusion is significantly lower for DOPC/DPPC/CHOL than for DOPC/SM/CHOL despite the similar main transition temperatures for DPPC and SM. This is a strong indication of a tighter interaction of CHOL with SM than with DPPC.

Low temperature region, 15 mol % CHOL

At 15 mol % CHOL the diffusion data by ^1H NMR shows a split into two diffusion coefficients at the same temperatures as for 30 mol %, but the relative amount of the slow component is very small (Fig. 2). The fast diffusion coefficient is close to that of DOPC/DPPC at all temperatures (Fig. 2, *left panel*, *solid line*), and it decreases monotonically at decreasing temperature, which is in contrast to the behavior shown in Fig. 1. Thus, we conclude that only small amounts of the l_o phase is formed at this composition. According to fluorescence microscopy 15 mol % CHOL is close to the l_d/s_o two-phase area and we cannot, therefore, exclude that part of the bilayers are forming a solid ordered gel phase, thereby becoming invisible in the diffusion experiments.

Both the diffusion components obtained by ^2H and ^{19}F NMR conform to the fast one measured by ^1H NMR. This is probably because the occurrence of a very small, slow diffusion component would be difficult to pick up by the CORE

analysis from the rather noisy spectra recorded by ^{2}H and ^{19}F NMR.

SUMMARY

We have shown that using isotopically labeled molecules in pfg-NMR is a powerful approach for investigations of dynamics and composition in raft-forming bilayer systems. Such NMR studies permit that each of the individual lipid species in the system can be studied, thus making it an ideal method for detailed investigations of lipid dynamics and partitioning in domains. ^{2}H and ^{19}F labeling at carefully chosen positions have so little influence on the molecular properties that the method approaches the noninvasive ideal.

At 30 mol % CHOL, large domains of the l_o phase form as evidenced by the slow exchange characteristics of the data. The lateral diffusion coefficients in the separate phases differ by a factor of ~5 and are independent of the lipid structure. There is a sudden increase in the fast proton diffusion coefficient as the temperature is dropped below T_{mix}, reflecting the changes in concentration as the system phase separates. DPPC is found to reside exclusively in the l_o phase, whereas DOPC and CHOL are distributed among both phases. The CHOL content is estimated to be 15 mol % in the l_d phase and to be 30–40 mol % in the l_o phase, in accordance with fluorescence studies. At 15 mol % CHOL, in the vicinity to the s_o/l_d two-phase region, only minor amounts of the l_o phase can be observed.

The technical support of Marcia Malmer (Northeastern Ohio Universities College of Medicine) is gratefully acknowledged.

This work was supported by the Swedish Research Council and the Knut and Alice Wallenberg Foundation.

REFERENCES

1. Simons, K., and E. Ikonen. 1997. Functional rafts in cell membranes. *Nature*. 387:569–572.
2. Brown, R. E. 1998. Sphingolipid organization in biomembranes: what physical studies of model membranes reveal. *J. Cell Sci.* 111: 1–9.
3. Brown, D. A. 2001. Seeing is believing: visualization of rafts in model membranes. *Proc. Natl. Acad. Sci. USA*. 98:10517–10518.
4. Silvius, J. R. 2003. Role of cholesterol in lipid raft formation: lessons from lipid model systems. *Biochim. Biophys. Acta*. 1610:174–183.
5. Simons, K., and W. L. Vaz. 2004. Model systems, lipid rafts, and cell membranes. *Annu. Rev. Biophys. Biomol. Struct*. 33:269–295.
6. Henderson, R. M., J. M. Edwardson, N. A. Geisse, and D. E. Saslowsky. 2004. Lipid rafts: feeling is believing. *News Physiol. Sci.* 19:39–43.
7. Mouritsen, O. G. 2005. Life—As a Matter of Fat. The Emerging Science of Lipidomics. Springer-Verlag, Berlin.
8. McConnell, H. M., and M. Vrljic. 2003. Liquid-liquid immiscibility in membranes. *Annu. Rev. Biophys. Biomol. Struct*. 32:469–492.
9. Ipsen, J. H., G. Kalström, O. G. Mouritsen, H. W. Wennerström, and M. J. Zuckermann. 1987. Phase equilibria in the phosphatidylcholine-cholesterol systems. *Biochim. Biophys. Acta*. 905:162–172.
10. Vist, M. R., and J. H. Davis. 1990. Phase equilibria of cholesterol/dipalmitoylphosphatidylcholine mixtures: ^{2}H nuclear magnetic resonance and differential scanning calorimetry. *Biochemistry*. 29:451–464.
11. Zajchowski, L. D., and S. M. Robbins. 2002. Lipid rafts and little caves. Compartmentalized signalling in membrane microdomains. *Eur. J. Biochem*. 269:737–752.
12. Isshiki, M., and R. G. Anderson. 1999. Calcium signal transduction from caveolae. *Cell Calcium*. 26:201–208.
13. Anderson, R. G., B. A. Kamen, K. G. Rothberg, and S. W. Lacey. 1992. Potocytosis: sequestration and transport of small molecules by caveolae. *Science*. 255:410–411.
14. Smart, E. J., G. A. Graf, M. A. McNiven, W. C. Sessa, J. A. Engelman, P. E. Scherer, T. Okamoto, and M. P. Lisanti. 1999. Caveolins, liquid-ordered domains, and signal transduction. *Mol. Cell. Biol*. 19:7289–7304.
15. Gustavsson, J., S. Parpal, M. Karlsson, C. Ramsing, H. Thorn, M. Borg, M. Lindroth, K. H. Peterson, K. E. Magnusson, and P. Stralfors. 1999. Localization of the insulin receptor in caveolae of adipocyte plasma membrane. *FASEB J*. 13:1961–1971.
16. Parpal, S., M. Karlsson, H. Thorn, and P. Stralfors. 2001. Cholesterol depletion disrupts caveolae and insulin receptor signaling for metabolic control via insulin receptor substrate-1, but not for mitogen-activated protein kinase control. *J. Biol. Chem*. 276:9670–9678.
17. Örtegren, U., M. Karlsson, N. Blazic, M. Blomqvist, F. H. Nystrom, J. Gustavsson, P. Fredman, and P. Stralfors. 2004. Lipids and glycosphingolipids in caveolae and surrounding plasma membrane of primary rat adipocytes. *Eur. J. Biochem*. 271:2028–2036.
18. Pohl, J., A. Ring, R. Ehehalt, H. Schulze-Bergkamen, A. Schad, P. Verkade, and W. Stremmel. 2004. Long-chain fatty acid uptake into adipocytes depends on lipid raft function. *Biochemistry*. 43:4179–4187.
19. Smart, E. J., Y. Ying, W. C. Donzell, and R. G. Anderson. 1996. A role for caveolin in transport of cholesterol from endoplasmic reticulum to plasma membrane. *J. Biol. Chem*. 271:29427–29435.
20. Bernardino de la Serna, J., J. Perez-Gil, A. C. Simonsen, and L. A. Bagatolli. 2004. Cholesterol rules: direct observation of the coexistence of two fluid phases in native pulmonary surfactant membranes at physiological temperatures. *J. Biol. Chem*. 279:40715–40722.
21. White, D. A. 1973. The phospholipid composition of mammalian tissue. *In* Form and Function of Phospholipids. G. Ansell, J. Hawthorne, and R. Dawson, editors. Elsevier, New York. 441–482.
22. Gandhavadi, M., D. Allende, A. Vidal, S. A. Simon, and T. J. McIntosh. 2002. Structure, composition, and peptide binding properties of detergent soluble bilayers and detergent resistant rafts. *Biophys. J*. 82:1469–1482.
23. Shaikh, S. R., A. C. Dumaual, L. J. Jenski, and W. Stillwell. 2001. Lipid phase separation in phospholipid bilayers and monolayers modeling the plasma membrane. *Biochim. Biophys. Acta*. 1512:317–328.
24. Radhakrishnan, A., and H. M. McConnell. 1999. Cholesterol-phospholipid complexes in membranes. *J. Am. Chem. Soc*. 121:486–487.
25. Yuan, C., J. Furlong, P. Burgos, and L. J. Johnston. 2002. The size of lipid rafts: an atomic force microscopy study of ganglioside GM1 domains in sphingomyelin/DOPC/cholesterol. *Biophys. J*. 82:2526–2535.
26. Rinia, H. A., M. E. Snel, J. P. J. M. Van der Eerden, and B. De Kruijff. 2001. Visualizing detergent-resistant domains in model membranes with atomic force microscopy. *FEBS Lett*. 501:92–96.
27. Lawrence, J. C., D. E. Saslowsky, J. M. Edwardson, and R. M. Henderson. 2003. Real-time analysis of the effects of cholesterol on lipid raft behavior using atomic force microscopy. *Biophys. J*. 84: 1827–1832.

28. Orädd, G., and G. Lindblom. 2004. NMR studies of macroscopically oriented bilayers. *Magn. Reson. Chem.* 42:123–131.

29. Veatch, S. L., I. V. Polozov, K. Gawrisch, and S. L. Keller. 2004. Liquid domains in vesicles investigated by NMR and fluorescence microscopy. *Biophys. J.* 86:2910–2922.

30. Veatch, S. L., and S. L. Keller. 2002. Organization in lipid membranes containing cholesterol. *Phys. Rev. Lett.* 89:268101-1–268101-4.

31. Dietrich, C., Z. N. Volovyk, M. Levi, N. L. Thompson, and K. Jacobson. 2001. Partitioning of Thy-1, GM1, and cross-linked phospholipid analogs into lipid rafts reconstituted in supported model membrane monolayers. *Proc. Natl. Acad. Sci. USA.* 98:10642–10647.

32. Dietrich, C., L. A. Bagatolli, Z. N. Volovyk, N. L. Thompson, M. Levi, K. Jacobson, and E. Gratton. 2001. Lipid raft reconstituted in model membranes. *Biophys. J.* 80:1417–1428.

33. Baumgart, T., S. T. Hess, and W. W. Webb. 2003. Imaging coexisting fluid domains in biomembrane models coupling curvature and line tension. *Nature.* 425:821–824.

34. Bacia, K., D. Scherfeld, N. Kahya, and P. Schwille. 2004. Fluorescence correlation spectroscopy relates rafts in model and native membranes. *Biophys. J.* 87:1034–1043.

35. Kahya, N., D. Scherfeld, K. Bacia, and P. Schwille. 2004. Lipid domain formation and dynamics in giant unilamellar vesicles explored by fluorescence correlation spectroscopy. *J. Struct. Biol.* 147:77–89.

36. Orädd, G., and G. Lindblom. 2004. NMR studies of lipid lateral diffusion in the DMPC/gramicidin D/water system: Peptide aggregation and obstruction effects. *Biophys. J.* 87:980–987.

37. Filippov, A., G. Orädd, and G. Lindblom. 2004. Lipid lateral diffusion in ordered and disordered phases in raft mixtures. *Biophys. J.* 86:891–896.

38. Filippov, A., G. Orädd, and G. Lindblom. 2003. The effect of cholesterol on the lateral diffusion of phospholipids in oriented bilayers. *Biophys. J.* 84:3079–3086.

39. Kauffman, J. M., P. W. Westerman, and M. C. Carey. 2000. Fluorocholesterols, in contrast to hydroxycholesterols, exhibit interfacial properties similar to cholesterol. *J. Lipid. Res.* 41:991–1003.

40. Tanner, J. E. 1970. Use of the stimulated echo in NMR diffusion studies. *J. Chem. Phys.* 52:2523–2526.

41. Stilbs, P., and K. Paulsen. 1996. Global least-squares analysis of large, correlated spectral data sets. Application to chemical kinetics and time-resolved fluorescence. *Rev. Sci. Instrum.* 67:4380–4386.

42. Stilbs, P., K. Paulsen, and P. C. Griffiths. 1996. Global least-squares analysis of large, correlated spectral data sets: application to component-resolved FT-PGSE NMR spectroscopy. *J. Phys. Chem.* 100:8180–8189.

43. Stilbs, P., and M. E. Moseley. 1978. Chemical exchange rates from Fourier transform measurements of nuclear spin-lattice relaxation in the rotating frame. Application to hindered internal rotation in urea. *J. Magn. Reson.* 31:55–61.

44. Almeida, P. F. F., W. L. C. Vaz, and T. E. Thompson. 1992. Lateral diffusion in the liquid phases of dimyristoilphosphatidylcholine/cholesterol bilayers: a free volume analysis. *Biochemistry.* 31:6739–6747.

45. Leathes, J. B. 1925. Role of fats in vital phenomena. *Lancet.* 208:853–856.

46. Megha, J. W., and E. London. 2004. Relationship between sterol/steroid structure and participation in ordered lipid domains (lipid rafts): Implications for lipid raft structure and function. *Biochemistry.* 43: 1010–1018.

47. Kärger, J., H. Pfeifer, and W. Heink. 1988. Principles and application of self-diffusion measurements by nuclear magnetic resonance. *In* Advances in Magnetic and optical resonance. W. S. Warren, editor. Academic Press, San Diego, CA. 1–89.

48. Veatch, S. L., and S. L. Keller. 2003. Separation of liquid phases in giant vesicles of ternary mixtures of phospholipids and cholesterol. *Biophys. J.* 85:3074–3083.

49. Sankaram, M. B., and T. E. Thompson. 1990. Interaction of cholesterol with various glycerophospholipids and sphingomyelin. *Biochemistry.* 29:10670–10675.